

Single photon ionization of hydrogen bonded clusters with a soft x-ray laser: $(\text{HCOOH})_x$ and $(\text{HCOOH})_y(\text{H}_2\text{O})_z$

S. Heinbuch

Department of Electrical and Computer Engineering, Colorado State University, Fort Collins, Colorado 80523 and NSF ERC for Extreme Ultraviolet Science and Technology, Colorado State University, Fort Collins, Colorado 80523

F. Dong

Department of Chemistry, Colorado State University, Fort Collins, Colorado 80523 and NSF ERC for Extreme ultraviolet Science and Technology, Colorado State University, Fort Collins, Colorado 80523

J. J. Rocca

Department of Electrical and Computer Engineering, Colorado State University, Fort Collins, Colorado 80523 and NSF ERC for Extreme Ultraviolet Science and Technology, Colorado State University, Fort Collins, Colorado 80523

E. R. Bernstein^{a)}

Department of Chemistry, Colorado State University, Fort Collins, Colorado 80523 and NSF ERC for Extreme Ultraviolet Science and Technology, Colorado State University, Fort Collins, Colorado 80523

(Received 7 February 2007; accepted 9 May 2007; published online 22 June 2007)

Pure, neutral formic acid $(\text{HCOOH})_{n+1}$ clusters and mixed $(\text{HCOOH})/(\text{H}_2\text{O})$ clusters are investigated employing time of flight mass spectroscopy and single photon ionization at 26.5 eV using a very compact, capillary discharge, soft x-ray laser. During the ionization process, neutral clusters suffer little fragmentation because almost all excess energy above the vertical ionization energy is taken away by the photoelectron, leaving only a small part of the photon energy deposited into the $(\text{HCOOH})_{n+1}^+$ cluster. The vertical ionization energy minus the adiabatic ionization energy is enough excess energy in the clusters to surmount the proton transfer energy barrier and induce the reaction $(\text{HCOOH})_{n+1}^+ \rightarrow (\text{HCOOH})_n\text{H}^+ + \text{HCOO}$ making the protonated $(\text{HCOOH})_n\text{H}^+$ series dominant in all data obtained. The distribution of pure $(\text{HCOOH})_n\text{H}^+$ clusters is dependent on experimental conditions. Under certain conditions, a magic number is found at $n=5$. Metastable dissociation rate constants of $(\text{HCOOH})_n\text{H}^+$ are measured in the range $(0.1-0.8) \times 10^4 \text{ s}^{-1}$ for cluster sizes $4 < n < 9$. The rate constants display an odd/even alternating behavior between monomer and dimer loss that can be attributed to the structure of the cluster. When small amounts of water are added to the formic acid, the predominant signals in the mass spectrum are still $(\text{HCOOH})_n\text{H}^+$ cluster ions. Also observed are the protonated mixed cluster series $(\text{HCOOH})_n(\text{H}_2\text{O})_m\text{H}^+$ for $n=1-8$ and $m=0-4$. A magic number in the cluster series $n=5, m=1$ is observed. The mechanisms and dynamics of formation of these neutral and ionic clusters are discussed. © 2007 American Institute of Physics. [DOI: 10.1063/1.2746036]

I. INTRODUCTION

Formic acid is the first organic acid that has been detected in interstellar ice and also plays a role in Earth's atmospheric chemistry. More recently it has been detected in the coma of comets.¹ It may be key in the formation of molecules such as glycine ($\text{NH}_2\text{CH}_2\text{COOH}$) and acetic acid (CH_3COOH) in the interstellar media.² Formic acid is the simplest of the carboxylic acids of the form RCOOH , in which R can be replaced by a number of substituents, and can serve as a model system for the properties of larger, more complex molecules. It has been analyzed thoroughly through theoretical calculations, mainly due to the abundance of available experimental data. Many of the experiments on formic acid involve electron impact (EI) ionization studies. EI causes substantial fragmentation, and neutral parent cluster

information is thereby lost. Our soft x-ray laser (26.5 eV photons) has proven itself in the past to be a gentle, single photon ionization source³⁻⁶ and we confirm that to be the case as well in the present study of formic acid.

Clusters are said to bridge the gap between gas and condensed phase behavior; extensive experiments have been conducted on formic acid clusters revealing the protonated cluster ion series of the form $(\text{HCOOH})_n\text{H}^+$, generated from a proton transfer reaction in the parent ion $(\text{HCOOH})_{n+1}^+$ directly following ionization of $(\text{HCOOH})_{n+1}^+$ at 26.5 eV. Experiments are reported by Lifshitz and Feng using EI ionization and unimolecular dissociation of the cluster series $(\text{HCOOH})_n\text{H}^+$ is observed and characterized.^{7,8} To accompany their experiments, the same group has performed *ab initio* calculations for the cluster ion series at the HF/4-31G# level.⁹ The optimized structures generated seem to agree well with experimental results, revealing that open

^{a)}Electronic mail: erb@lamar.colostate.edu

chain structures are favored for cluster values $n \leq 5$, and chain structures terminated by cyclic dimer units are favored for $n \geq 6$. The infrared photodissociation spectra of protonated formic acid clusters were studied by Inokuchi and Nishi.¹⁰ Their studies reveal two free OH stretching vibrations for the $n=2, 3$ species indicating a chain structure open on both ends. The $n=4$ and 5 ions reveal only one free OH stretching vibration, signifying that the chain may be terminated on one end by a cyclic dimer while the other end remains open. The $n=7$ ion species does not possess a free OH vibrational band, implying that both ends of the chain structure are terminated by cyclic dimers.¹⁰ They too provide density functional theory (DFT) calculations that corroborate their experimental data.

The aqueous protonated cluster ion series denoted as $(\text{HCOOH})_n(\text{H}_2\text{O})_m\text{H}^+$ has also been extensively researched. Feng and Lifshitz have reported formic acid/water cluster series studies in which they observe a particularly abundant protonated cluster ion of the form $(\text{HCOOH})_5(\text{H}_2\text{O})\text{H}^+$.⁷ This cluster size may be referred to as a “magic number.” Employing collisionally activated dissociation, they observe that clusters with smaller n values favor water molecule loss and those with larger n values favor formic acid molecule loss. The data suggests that a critical cluster size, n , exists below which an $(\text{HCOOH})\text{H}^+$ ion core is preferred rather than a $(\text{H}_2\text{O})\text{H}^+$ ion core. Above this value the opposite is true. On the basis of *ab initio* molecular orbital calculations at the HF-/4-31G# level,¹¹ they conclude that the proton switch occurs between the values $n=3$ and 4. Inokuchi and Nishi report infrared photodissociation spectroscopy data for protonated formic acid water clusters $(\text{HCOOH})_n(\text{H}_2\text{O})_m\text{H}^+$.^{10,12} In the $m=1$ series, they find a water asymmetric OH stretch vibration for clusters $n=1-3$, which disappears for the $n=4$ and 5 clusters. Their results imply that the ion core switches from $(\text{HCOOH})\text{H}^+$, for $n=1-3$, to $(\text{H}_2\text{O})\text{H}^+$ for $n=4$ and 5. They also suggest that the $n=5, m=1$ cluster ion has a stable cyclic type structure in which the $(\text{H}_2\text{O})\text{H}^+$ ion is fully surrounded and secured by five formic acid molecules. This is the reason for the magic number at $n=5, m=1$, according to Ref. 12.

In the present study, formic acid and mixed formic acid/water clusters are accessed by single photon ionization with a 26.5 eV (46.9 nm) soft x-ray laser. The distributions of neutral $(\text{HCOOH})_{n+1}$ and $(\text{HCOOH})/(\text{H}_2\text{O})$ clusters are detected. Metastable dissociation rate constants for $(\text{HCOOH})_n\text{H}^+$ cluster ions are measured in the range of $4 \leq n \leq 9$. The rate constants display an odd/even alternating behavior between monomer and dimer loss that can be attributed to the structure of the cluster. After proton transfer, $(\text{HCOOH})_n\text{H}^+$ cluster ions are the dominant products in the photoionization of neutral $(\text{HCOOH})_{n+1}$ clusters using a single photon of 26.5 eV energy for ionization. Compared with electron impact techniques, $(\text{HCOOH})_n\text{H}^+$ clusters suffer only a small dissociation by the present single photon ionization and thus a nearly accurate neutral cluster distribution is detected by time of flight mass spectroscopy (TOFMS). Similar results, with regard to soft x-ray laser single photon ionization, are found for other van der Waals and hydrogen bonded clusters, as well as metal and metal

oxide clusters.³⁻⁶ The neutral cluster distribution $(\text{HCOOH})_{n+1}$, as observed through $(\text{HCOOH})_n\text{H}^+$ ions, shows an anomalous relative intensity peak (magic number) at $n=5$ (for certain conditions). For the neutral $\text{HCOOH}/\text{H}_2\text{O}$ cluster series, the protonated mixed cluster series $(\text{HCOOH})_n(\text{H}_2\text{O})_m\text{H}^+$ for $n=1-8$ and $m=0-4$ is observed. A magic number in the cluster series $n=5$, at $m=1$ is observed. The mechanism for mixed cluster formation is discussed in detail in this report.

II. EXPERIMENTAL PROCEDURES

The experimental apparatus and soft x-ray laser have been described in previous publications from this laboratory³⁻⁶ and therefore only a general outline of the experimental scheme will be presented in this report. A tabletop soft x-ray laser (26.5 eV photons) is used as the single photon ionization source.¹³ The laser emits pulses of approximately 1 ns duration with an energy of approximately 10 $\mu\text{J}/\text{pulse}$ at a repetition rate of up to 12 Hz. Laser action is produced by electron impact ionization to generate Ne-like argon ions in the plasma of a fast capillary discharge.^{14,15} A (linear/reflectron) TOFMS is used as a mass analyzer. A pair of mirrors placed in Z-fold configuration just before the ionization region of the TOFMS provides alignment capability and focus for the laser beam with respect to the molecular beam at the ionization source. The Z-fold transmissivity is about 10% and thus the ionization point in the TOFMS receives about 1 $\mu\text{J}/\text{pulse}$ laser energy. Since the 26.5 eV photons from the soft x-ray laser are able to ionize the He carrier gas employed in the supersonic expansion discussed below, the microchannel plate (MCP) mass detector voltage is gated to reduce the gain of the plates when He^+ ions arrive at the MCP in order to prevent detector circuit overload and saturation.

Pure neutral $(\text{HCOOH})_{n+1}$ clusters are generated in a supersonic expansion of HCOOH/He mixed gas created by flowing helium through a formic acid reservoir at a backing pressure up to 150 psi. The mixture expands into vacuum from a pulsed nozzle (200 μm diameter opening). A mixed $\text{HCOOH}/\text{H}_2\text{O}$ gas is obtained by flowing He at pressures of 40 or 150 psi through a reservoir containing a 2% or 98% liquid formic acid/water mixture at room temperature. Mixed $\text{HCOOH}/\text{H}_2\text{O}$ clusters are generated in a molecular beam by expanding the gas mixture into a vacuum chamber. The molecular beam is collimated by a skimmer with a 2.0 mm diameter aperture at its apex, located approximately 2 cm downstream from the nozzle. Chamber pressure in the field free and detector regions of the TOFMS is on the order of 10^{-6} Torr during the experiment. Experiments are conducted to ensure that collision induced dissociation of cluster ions is negligible. The pressure in the beam at the ionization region (approximately 10^{-5} Torr) is too low to cause collision induced ionization of $(\text{HCOOH})_{n+1}$.

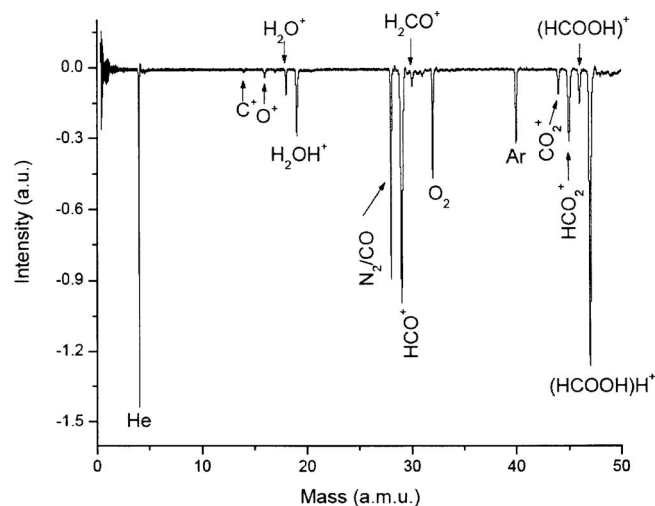
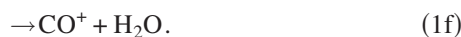
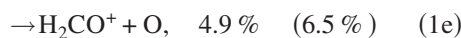
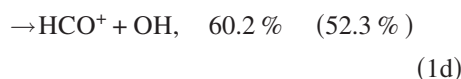
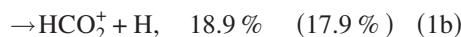
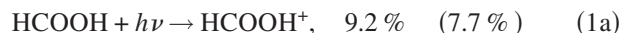


FIG. 1. Mass spectrum of formic acid monomer ionized by a 26.5 eV soft x-ray laser. The feature at 47 amu, $(\text{HCOOH})\text{H}^+$, is due to proton transfer generated fragmentation of the formic acid dimer cation.

III. RESULTS

A. Photoionization of formic acid monomer, dimer, and clusters

Figure 1 depicts the mass spectrum of the formic acid monomer ionized by 26.5 eV photons. The products HCOOH^+ , HCO_2^+ , CO_2^+ , HCO^+ , and H_2CO^+ are observed from the photolysis of the HCOOH molecule. The product channels are thus



The HCO^+ ion is the major photoionization channel in which the HCOOH molecule loses an OH radical. The undissociated formic acid ion channel yields about 9.2% of the product species. The product CO^+ cannot be assigned since a big background signal of N_2 is detected at the same mass number of 28. If the clusters are formed at a condition of 2% HCOOH and 98% H_2O , the distribution of formic acid clusters changes so that only the formic acid dimer is present, and $(\text{H}_2\text{O})_n$ and mixed $(\text{H}_2\text{O})_n(\text{HCOOC})_m$ clusters dominate the mass spectrum, as discussed below. These latter branching ratios, shown in parentheses, do not change significantly with the exception of the CO_2^+ channel. This may be caused by variable residual CO_2 in the vacuum chamber or in the $\text{H}_2\text{O}/\text{HCOOH}$ mixture. Under the two conditions, the ratios of $\text{HCOOH}^+/\text{HCO}_2^+$ and $\text{HCOOH}^+/\text{HCO}^+$ are similar. This comparison emphasizes that the observed monomer frag-

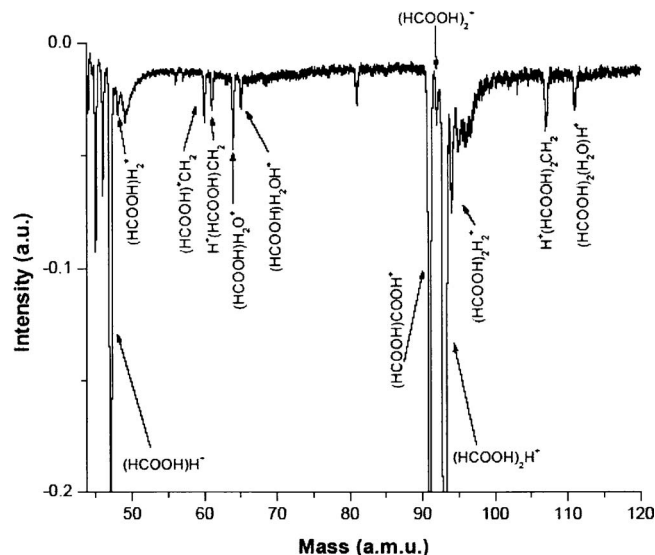
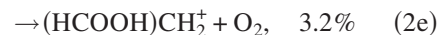
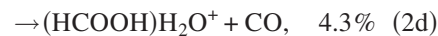
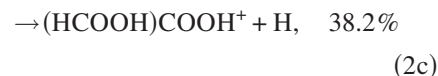
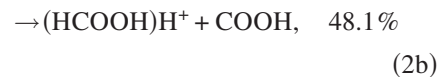


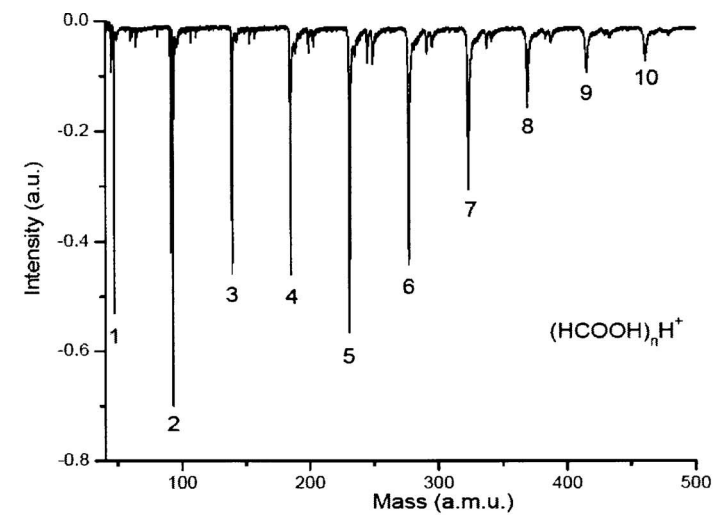
FIG. 2. Mass spectrum of formic acid dimer ionized by a 26.5 eV soft x-ray laser. The $(\text{HCOOH})_2\text{H}^+$ features arise from the proton transfer reaction in the $(\text{HCOOH})_3^+$ cluster.

ments are not derived from large $(\text{HCOOH})_n$ cluster fragmentation.

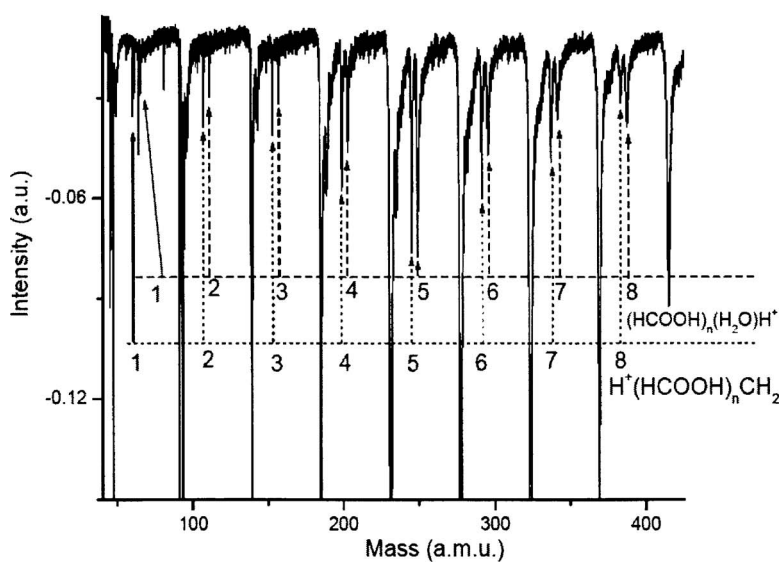
Figure 2 depicts the mass spectrum of the formic dimer for which the products $(\text{HCOOH})_2^+$, $(\text{HCOOH})\text{COOH}^+$, $(\text{HCOOH})\text{H}_2\text{O}^+$, $(\text{HCOOH})\text{CH}_2^+$, $(\text{HCOOH})\text{H}_2^+$, and $(\text{HCOOH})\text{H}^+$ are observed from the photoionization of the neutral $(\text{HCOOH})_2$ dimer. The product channels are identified as



The $(\text{HCOOH})\text{H}^+$ species is the major photoionization product and stems from the proton transfer reaction of the dimer ion $(\text{HCOOH})_2^+$ following ionization. The undissociated formic acid dimer ion product, generated directly from ionization of the neutral dimer, yields about 3.3% of the product species. Channel (2d), loss of a CO molecule to produce $(\text{HCOOH})\text{H}_2\text{O}^+$, is found to be an actual dissociation channel and not the result of excess water in the system. This fact is tested during experiments of mixed formic acid/water clusters. If excess water is added to the system, the relative ratio of dissociation channel (2d) does not increase, signifying that it is an actual channel of dissociation following photoionization of the formic acid dimer. An additional minor feature associated with the formic acid dimer appears at



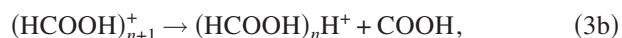
(a)



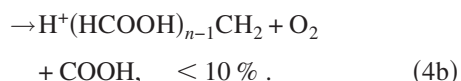
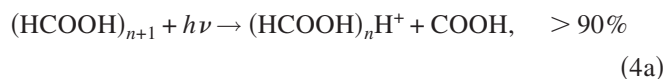
(b)

FIG. 3. (a) Mass spectrum showing the dominant protonated formic acid cluster series $(\text{HCOOH})_n\text{H}^+$. Note that the intensity of the $(\text{HCOOH})\text{H}^+$ signal is reduced by MCP gating because it saturates the detection system at the normal high voltage, gain setting. (b) An expanded scale view of revealing the cluster ion series $(\text{HCOOH})_n(\text{H}_2\text{O})\text{H}^+$ and $(\text{HCOOH})_n\text{CH}_2\text{H}^+$.

the $(\text{HCOOH})\text{CH}_2^+$ mass channel [Eq. (2e)], as shown in Fig. 2. Besides proton transfer,



which is the dominant product channel for clusters $n \geq 2$ as displayed in Fig. 3(a), this minor photoionization feature [Eq. (2e)] is the only other channel for dissociation following photoionization observed for larger clusters as shown in Fig. 3(b). The product channels for clusters $n \geq 3$ are thus



One also notes a series of mixed formic acid-water clusters, $(\text{HCOOH})_n\text{H}_2\text{O}^+$, due to residual water in the expansion gases, nozzle, or vacuum system. We do not observe the

same fragment channels for larger clusters as the monomer or dimer except for the case in which the loss of COOH is present. In fact, the intensity of $(\text{HCOOH})\text{H}^+$ is large enough to saturate the MCP detector, and we reduce the intensity of this mass channel by gating the MCP timing. Therefore, in Fig. 3(a), the $(\text{HCOOH})\text{H}^+$ signal is smaller than the $(\text{HCOOH})_2\text{H}^+$. In addition, the intensities of $(\text{HCOOH})_n\text{CH}_2^+$ and $(\text{HCOOH})_n\text{H}_2\text{O}^+$ signals obviously follow the change of the cluster distribution as shown in Figs. 3(a) and 3(b).

B. Distribution of neutral $(\text{HCOOH})_{n+1}$ clusters and mixed $(\text{HCOOH})/(\text{H}_2\text{O})$ clusters

Figure 4 displays a sequence of linear TOF mass spectra of $(\text{HCOOH})_n\text{H}^+$ clusters photoionized by a single photon of 26.5 eV energy from the soft x-ray laser. The spectra reveal the size distribution of the cluster ions as they are generated in the ionization/extraction region of the TOFMS on a time scale of less than 1 μs after ionization, as the laser/nozzle time separation is varied. The spectra, as viewed from top to bottom of Fig. 4, differ by an increased timing delay between

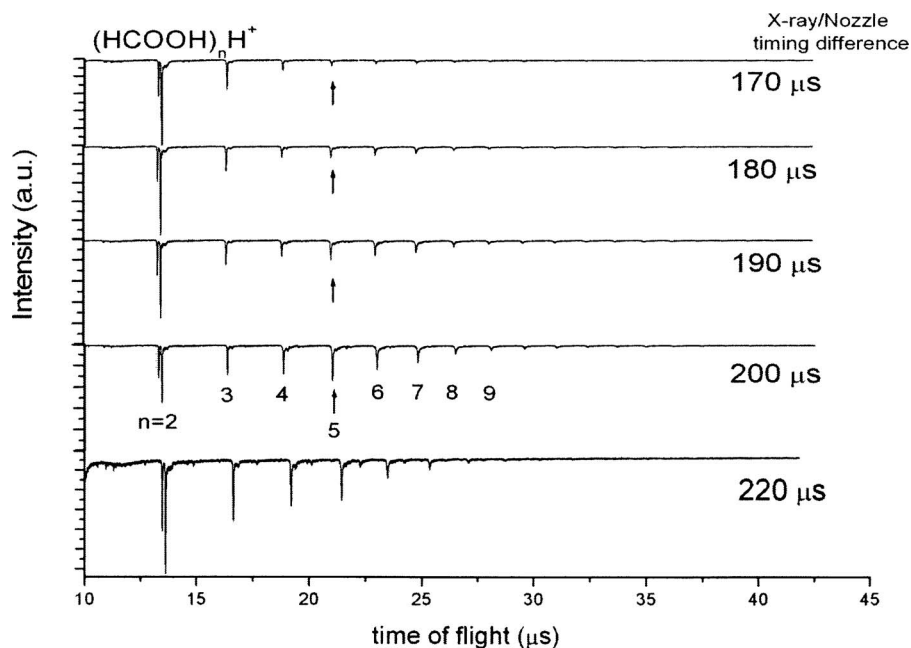


FIG. 4. High resolution mass spectra sequence of HCOOH clusters that are generated by expansion of mixed gas HCOOH/He at 150 psi backing pressure. Cluster ions $(\text{HCOOH})_n\text{H}^+$ dominate the mass spectrum. A magic number at $n=5$ develops as conditions are changed. The time axis refers to the delay between nozzle opening and laser firing.

the soft x-ray laser and pulsed gas nozzle. At $170 \mu\text{s}$ delay time, the intensity of clusters decreases approximately exponentially as a function of increasing cluster ion size n . As the timing delay is increased, one witnesses the emergence of a magic number in the cluster distribution. The distribution is dominated by protonated cluster ions of the form $(\text{HCOOH})_n\text{H}^+$ ($2 \leq n \leq 15$) with an intensity anomaly at $n=5$. After $200 \mu\text{s}$, the magic number at $n=5$ decreases until the cluster distribution resembles the distribution at $170 \mu\text{s}$; it decreases approximately exponentially with no intensity anomalies. Such a result could not arise if major cluster fragmentation were associated with 26.5 eV ionization.

Mixed HCOOH/ H_2O clusters are generated by expanding He gas and formic acid/water into the vacuum chamber at room temperature under two different experimental conditions: (1) 2% H_2O mixed with 98% HCOOH at 150 psi backing pressure; and (2) 2% HCOOH mixed with 98% H_2O at 40 psi backing pressure. Figure 5 shows a mass spectrum of mixed HCOOH/ H_2O clusters formed under condition (1). At this high backing pressure, high HCOOH content condition, $(\text{HCOOH})_n\text{H}^+$ cluster ions dominate the spectrum, and pure water clusters are not observed. Also produced in the mass spectrum are the protonated series $(\text{HCOOH})_n(\text{H}_2\text{O})_m\text{H}^+$ for $n=1-8$, and $m=0-4$. The unprotonated series are not observed. Figure 6 displays a plot of the intensity of the mixed cluster as a function of the number of HCOOH molecules, n , for $0 \leq m \leq 4$. In the cluster series with $m=0$, the intensity decreases roughly exponentially with increasing cluster size. At $m=1$, however, we observe a magic number at $n=5$. In the series $m=2$, the intensity for $n=6$ is slightly larger than its neighbors and for $m > 2$, the intensity is nearly constant for all n .

If the concentration of HCOOH and the backing pressure are reduced to that of condition (2) (low concentration and pressure), the dominant signal in the mass spectrum changes from $(\text{HCOOH})_n\text{H}^+$ to $(\text{HCOOH})(\text{H}_2\text{O})_m\text{H}^+$ ($m=0-16$), and pure water clusters are observed, as illustrated in Fig. 7. The

series $(\text{HCOOH})_n(\text{H}_2\text{O})_m\text{H}^+$ for $n=0-3$, and $m=0-16$ are also observed. Figure 8 displays a plot of the intensity of the clusters as a function of the number of H_2O molecules, m , for $n=0-3$ HCOOH molecules. In the cluster series with $m=0$, the intensity decreases roughly exponentially with increasing cluster size. No mixed clusters are observed to have relative intensity anomalies; magic numbers in any of the cluster series for low concentration and pressures of HCOOH are not found.

C. Metastable dissociation rate constants for $(\text{HCOOH})_n\text{H}^+$ cluster ions

Figure 9 presents a reflectron TOF mass spectrum indicating the population distribution of cluster ions formed in

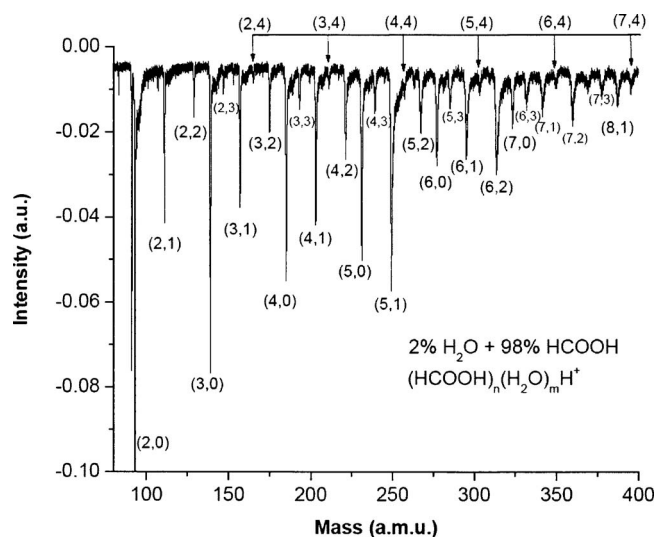


FIG. 5. High resolution mass spectrum of mixed HCOOH/ H_2O clusters that is generated by flowing He gas at 150 psi through a 2% H_2O 98% HCOOH liquid mixture. Cluster ions $(\text{HCOOH})_n(\text{H}_2\text{O})_m\text{H}^+$ are observed for $n=1-8$ and $m=1-4$. The development of a magic number at $n=5$, $m=1$ is observed.

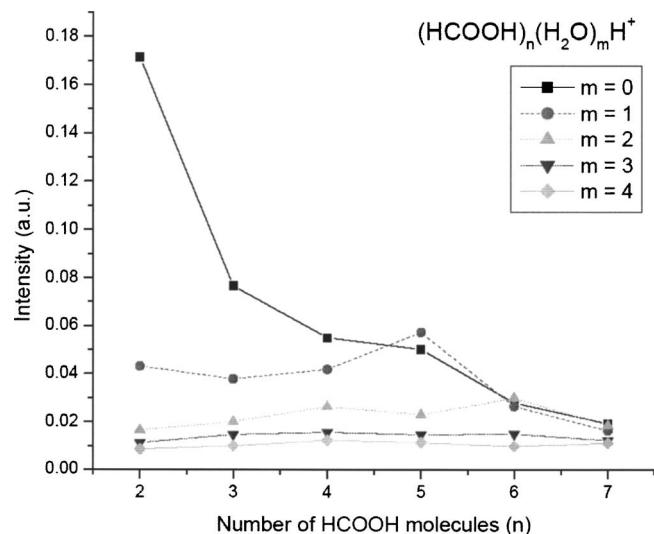
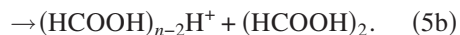
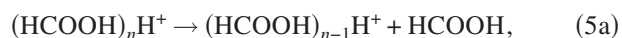


FIG. 6. Plot of the intensity as a function of the number of HCOOH molecules (n) for the series $(\text{HCOOH})_n(\text{H}_2\text{O})_m\text{H}^+$ for a constant number of water molecules (m). m is increased from 0 to 4. A magic number for $n=5$, $m=1$ is observed as well as a slight increase in intensity for $n=6$, $m=2$.

the first field free region of the TOFMS. Daughter ions are produced from their parent ions by metastable dissociation reactions in the drift tube. Both the loss of a monomer and a dimer from the parent cluster ion to generate the daughter ion are evident,



The metastable dissociation process of losing one dimer to obtain reaction (5b) may also be identified as a process of losing two monomers; however, it has been demonstrated in our previous work³⁻⁶ that the loss of only one neutral molecule from a metastable cluster ion by unimolecular dissociation can occur on a microsecond time scale using single photon ionization of our 26.5 eV laser. So in this case, losing

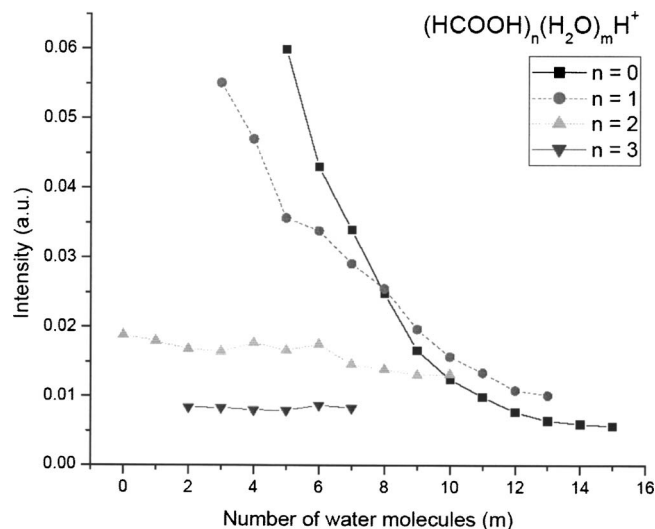


FIG. 8. A plot of intensity as a function of the number of H_2O molecules (m) for the series $(\text{HCOOH})_n(\text{H}_2\text{O})_m\text{H}^+$ for a constant number of formic acid molecules (n). n is increased from 0 to 3. No intensity anomalies are observed.

one dimer unit, not two monomers, from the parent ion is probably correct.

The unimolecular metastable dissociation rate constants for the $(\text{HCOOH})_n\text{H}^+$ cluster ion dissociation to generate $(\text{HCOOH})_{n-1,2}\text{H}^+$ can be calculated as

$$k = -(1/t)\ln[1 - I_D/(I_D + I_P)], \quad (6)$$

in which I_D and I_P are the intensities of the dissociated daughter ion and the undissociated parent ions, respectively, and t is the time of flight of the parent ion in the first field free region of the reflectron TOFMS. For the present apparatus this is about 60% of the total flight time for the reflectron mode TOFMS. Figure 10 shows that these rate constants, for cluster ions $4 \leq n \leq 9$, fall between 0.1 and $0.8 \times 10^4 \text{ s}^{-1}$. For the cluster value $n=4$, the k value for the loss of a dimer is favored over loss of a monomer by a factor of 5. For the cluster $n=5$, the loss of a monomer is favored over

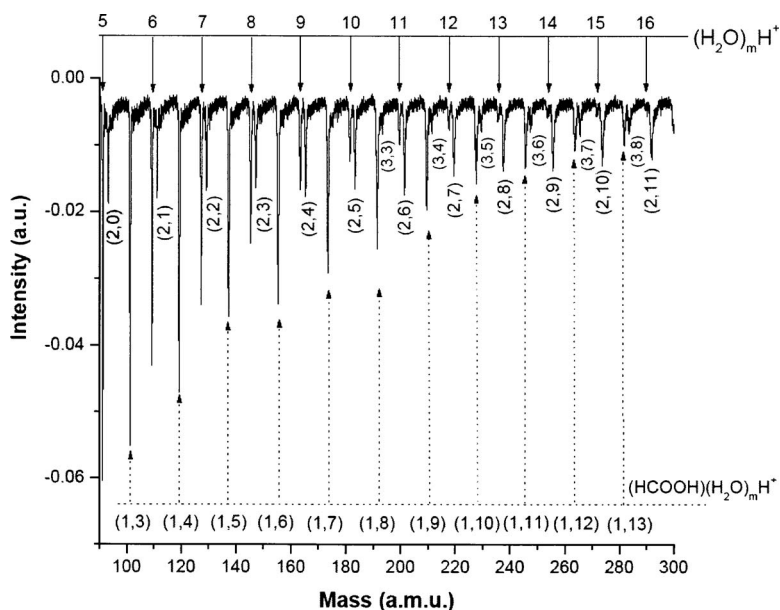


FIG. 7. High resolution mass spectrum of mixed $\text{HCOOH}/\text{H}_2\text{O}$ clusters that is generated by flowing He gas at 40 psi through a 2% HCOOH , 98% H_2O liquid mixture. Cluster ions $(\text{HCOOH})_n(\text{H}_2\text{O})_m\text{H}^+$ are observed for $n=0-3$ and $m=0-16$.

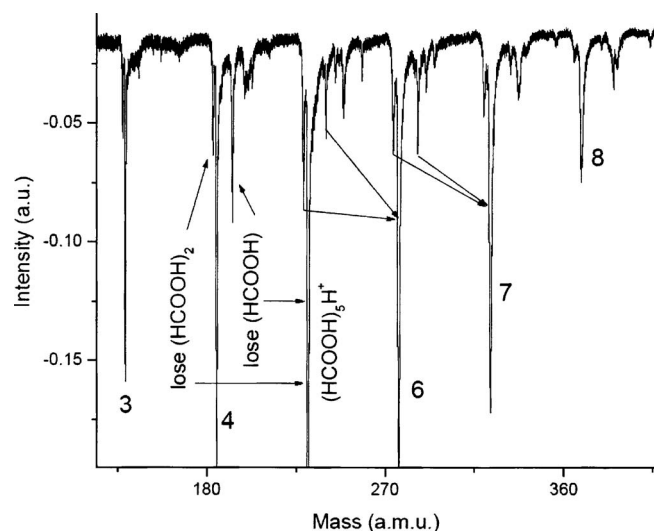


FIG. 9. High resolution reflectron TOF mass spectrum of $(\text{HCOOH})_n\text{H}^+$ clusters. Metastable dissociation of $(\text{HCOOH})_n\text{H}^+$ cluster ions in the field free region is observed. The loss of monomer and dimer units from the parent ion $(\text{HCOOH})_n\text{H}^+$ is displayed.

that of dimer. For $n=6-9$, dimer loss is favored over monomer loss but an oscillating behavior in the rate constant for odd and even clusters is observed. The rate constant for loss of a monomer is larger for odd numbered clusters ($n=5,7,9$), and the rate constant for loss of a dimer is larger for even numbered clusters ($n=4,6,8$).

IV. DISCUSSION

A. Photolysis of formic acid monomer and clusters

Photodissociation of formic acid in the gas phase has been studied extensively at 220–193 nm.¹⁶ A direct dissociation to $\text{HCO}+\text{OH}$ at the S_1 state was found to be a dominant pathway with a quantum yield of 0.7–0.8. A small amount of CO and CO_2 was also observed as a result of internal conversion to the ground state. Similar photolysis pathways are observed when 26.5 eV light is employed to ionize the for-

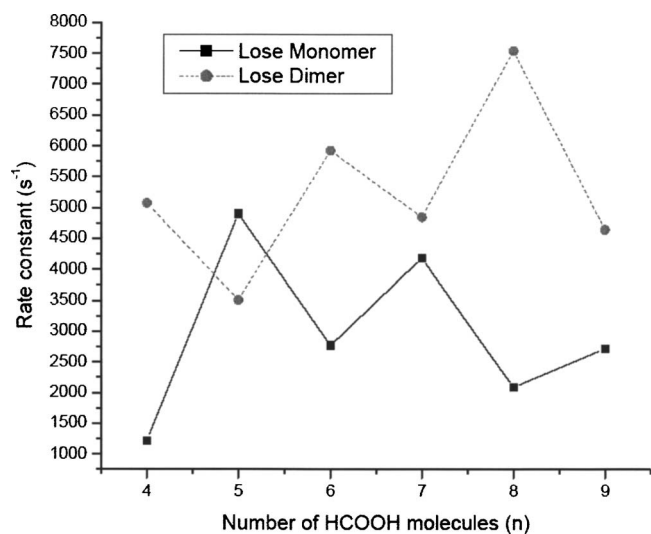


FIG. 10. A plot of metastable dissociation rate constants for $(\text{HCOOH})_n\text{H}^+$ cluster ions as a function of the cluster size, n .

mic acid monomer. The HCO^+ , CO_2^+ are observed in the mass spectrum of Fig. 1. The channel HCO^++OH is identified as the main photodissociation channel with quantum yield of 0.60. A minor channel of $\text{H}_2\text{CO}^++\text{O}$ is identified experimentally for the first time. Based on theoretical calculation,¹⁷ this path needs 180 kcal/mol energy above ground state to enable this reaction occur. Our 26.5 eV, soft x-ray laser has enough energy to excite a formic acid molecule to this high excited state during the ionization process.

Dissociation following photoionization of the formic acid dimer is studied for the first time. $(\text{HCOOH})\text{H}^+$ is the main product generated from the neutral dimer by a proton transfer reaction after ionization by 26.5 eV radiation. A second dissociation product, $(\text{HCOOH})\text{COOH}^+$, generated by loss of a H atom, has a high quantum yield, 0.38. The minor pathways to produce CO and CO_2 are also identified by observation of fragments $(\text{HCOOH})\text{H}_2\text{O}^+$ and $(\text{HCOOH})\text{H}_2^+$, respectively. An interesting feature in the dissociation of the dimer is the absence of a channel containing the loss of an OH, which is the main channel for dissociation following photoionization of the monomer HCOOH . This dissociation suggests that the neutral formic acid dimer contains a double hydrogen bond, with no free OH available for dissociation, and not an open chain structure. Neutral formic acid clusters are hydrogen bonded in nature, and the dimer has been experimentally established to possess a cyclic C_{2h} structure in the gas phase with two hydrogen bonds of 29.3 kJ/mol each;¹⁸ these bonds are nearly linear and are of the form $\text{O}-\text{H}\cdots\text{O}$.

The dissociation channel losing O_2 to produce $\text{H}^+(\text{HCOOH})_{n-1}\text{CH}_2$ is observed for larger clusters with small quantum yields, about 0.1; however, the dissociation channels for losing OH (yield, 0.60) and H (yield, 0.38), which are the main channels for the monomer and dimer, are not observed for larger clusters. The absence of these channels for larger clusters (>2) indicates that no free OH moiety exists in the structure of neutral formic acid clusters. Based on DFT^{19,21} calculations, the trimer structure with the lowest energy consists of the cyclic dimer bonded to a monomer by an $\text{O}-\text{H}\cdots\text{O}$ and a $\text{C}-\text{H}\cdots\text{O}$. Also, the lowest energy structure of the tetramer contains a pair of dimers held together by two weak $\text{C}-\text{H}\cdots\text{O}$ bonds.^{20,21} For neutral formic acid clusters, the general trend for $n \leq 5$ seems to be that the lowest energy structures favor rings or chains made up of the lowest energy dimers, and trimers in combination with monomers. Thus the DFT calculated structures are in agreement with the observed photoionization/dissociation chemistry. Additionally, larger clusters possess many more vibrational degrees of freedom that can absorb any excess energy deposited in the cluster, rendering fragmentation a slow process in general, and closing certain low probability channels. Similar behavior is observed in the study of $(\text{SO}_2)_n$ (Ref. 4) and $(\text{CO}_2)_n$ (Ref. 5) clusters.

The dissociation channels given in Eqs. (1) and (2) discussed above occur for higher excited electronic states of the monomer and clusters pumped by 26.5 eV radiation; however, these channels are apparently very minor features for larger clusters. In our previous studies of $(\text{SO}_2)_n$ clusters,⁴ a large dissociation to ionization ratio at electronically excited

states of the ion is observed for the SO_2 monomer, $I[\text{SO}^+]/I[\text{SO}_2^+]=1.1$. This ratio decreases to $I[(\text{SO}_2)_{n \geq 5}\text{SO}^+]/I[(\text{SO}_2)_{n \geq 5}^+] < 0.1$ as cluster size increases. This behavior is also observed in the studies of other clusters.^{3,5} Compared with EI, dissociation by 26.5 eV single photon ionization is much smaller. For example, the dissociation branching ratios of $(\text{CO}_2)_n$ clusters is up to 0.5 for EI ionization, but < 0.1 for 26.5 eV ionization.⁵ The mechanism for this behavior may be that as the excited ion states become more delocalized due to interactions in the cluster (charge delocalization), their absorption cross section for the reaction $I+h\nu \rightarrow I^{*+} + e^-$ decreases. Such behavior is found for charge transfer transitions in extended systems, in general.

Another issue that can be argued is that these observed dissociation channels could arise from the fragmentation of larger clusters. Three pieces of evidence arise from our data that can help address this issue. First, the branching ratios for HCO_2^+ , HCO^+ , and H_2CO^+ are not changed under two different experimental conditions of cluster formation. For the pure formic acid/He expansion, the $(\text{HCOOH})_n\text{H}^+$ cluster distribution can be observed for $n \sim 1-10$, while only the formic acid dimer is observed if water is added to the formic acid liquid generating a concentration of 2% $\text{HCOOH}/98\% \text{H}_2\text{O}$ for the He carrier gas expansion. If fragmentation occurs for larger clusters, the branching ratios of HCO_2^+ , HCO^+ and H_2CO^+ should increase for the pure formic acid expansion, since large clusters are present in this instance only. Nonetheless, the fragment branching ratios remain the same for both cases. Second, the dissociation product signals $\text{H}^+(\text{HCOOH})\text{CH}_2$ and $(\text{HCOOH})\text{H}_2\text{O}^+$ are smaller than dissociation product signals $\text{H}^+(\text{HCOOH})_n\text{CH}_2$ and $(\text{HCOOH})_n\text{H}_2\text{O}^+$ for $n > 2$, indicating that fragmentation from larger clusters does not contribute greatly to the $\text{H}^+(\text{HCOOH})\text{CH}_2$ and $(\text{HCOOH})\text{H}_2\text{O}^+$ signal intensities. Also the intensity of the $\text{H}^+(\text{HCOOH})_n\text{CH}_2$ and $(\text{HCOOH})_n\text{H}_2\text{O}^+$ fragment signals obviously follows, the change in intensity for the parent signal, as shown in Fig. 3: that is, the fragment intensity increases for $n=2-5$ and then decreases for $n > 5$. Thus, $\text{H}^+(\text{HCOOH})\text{CH}_2$ and $(\text{HCOOH})\text{H}_2\text{O}^+$ must be generated from the formic acid dimer. Another main dissociation product, $(\text{HCOOH})\text{COOH}^+$, can also only result from the dimer since dissociation products $(\text{HCOOH})_n\text{COOH}^+$ for $n > 2$ are not observed in our experiment. If large clusters generate the fragment $(\text{HCOOH})\text{COOH}^+$, one should observe a distribution of $(\text{HCOOH})_n\text{COOH}^+$ ($n > 2$) in the cluster distribution. This is not the case. Third, the distribution of cluster ions is dependent on the neutral cluster structures. As shown in Fig. 3, the intensities of $(\text{HCOOH})\text{H}^+$ and $(\text{HCOOH})_5\text{H}^+$ clusters are larger than their neighbors. This is due to the stable structure of $(\text{HCOOH})_2$ and $(\text{HCOOH})_6$. The formic acid dimer mainly consists of a double hydrogen bonded structure in formic acid vapor.¹⁹ If one assumes that the large clusters fragment to the smaller clusters during the 26.5 eV ionization process, one should observe the cluster distribution intensity decrease with increasing cluster size. One should not observe the magic number at $(\text{HCOOH})_5\text{H}^+$ in the cluster distribution since a 26.5 eV photon has enough energy to fragment any large cluster to the monomer after ionization.

Since we do observe a magic number, we consider that formic acid clusters do not suffer serious fragmentation during 26.5 eV ionization.

B. Distribution of $(\text{HCOOH})_n$ clusters and mixed $\text{HCOOH}/\text{H}_2\text{O}$ clusters

We have learned from studies of H_2O , CH_3OH , NH_3 ,³ SO_2 ,⁴ CO_2 ,⁵ and metal oxide clusters,⁶ as well as this study of HCOOH , that 26.5 eV photons ionize van der Waals and hydrogen bonded clusters such that very little energy above the vertical ionization energy (VIE) remains in the cluster. Cluster fragmentation in the ionization region of the mass spectrometer (less than 1 μs following ionization) is driven in most instances by the energy difference between cluster VIE and adiabatic ionization energy (AIE) or the energy difference between VIE and the barrier to the proton transfer/dissociation reaction following ionization. The proton transfer/dissociation reaction is typically quite exothermic and this energy can also be used in part to fragment (metastable fragmentation, typically) the cluster. The protonated cluster $(\text{HCOOH})_n\text{H}^+$ signal is dominant in the mass spectra as the VIE minus the AIE is always enough energy to drive a proton transfer reaction following ionization. The proton transfer reaction cannot be avoided for hydrogen bonded clusters even if ionization takes place at the VIE threshold, and is not a result of a 26.5 eV photon inputting excess energy (above the cluster VIE) into the cluster. The only additional fragmentation beyond that driven by proton transfer in the reaction $(\text{HA})_{n+1}^+ \rightarrow (\text{HA})_n\text{H}^+ + \text{A}$ is metastable fragmentation³⁻⁶ after the ion has traveled out of the ionization region and gone into the flight tube of the TOFMS. This fragmentation occurs at times greater than 1 μs following the laser ionization pulse and is detected by reflectron TOFMS.³⁻⁶ We will discuss this latter issue in Sec. IV C.

As illustrated in Fig. 4, signals for $(\text{HCOOH})_n\text{H}^+$ cluster ions dominate the mass spectrum for all n due to a proton transfer reaction following ionization. The signal for the fragmentation series $\text{H}^+(\text{HCOOH})_{n-1}\text{CH}_2$ becomes increasingly weak over the range $n=1-8$. For 26.5 eV single photon ionization, the summed relative intensity ratios for fragment ions with respect to the $(\text{HCOOH})_n\text{H}^+$ main feature is < 0.1 for all values of n . These results, in conjunction with linear TOFMS data, strongly suggest that the neutral cluster distribution, $(\text{HCOOH})_{n+1}$, is quite similar to the observed $(\text{HCOOH})_n\text{H}^+$ distribution. In the experiment, the cluster distribution is related to the timing delay between the ionization laser pulse and pulsed gas nozzle trigger. Under certain conditions, the $(\text{HCOOH})_5\text{H}^+$ cluster displays an intensity anomaly (see Fig. 4). The $(\text{HCOOH})_5\text{H}^+$ cluster is generated from the neutral cluster $(\text{HCOOH})_6$ in the molecular beam by a proton transfer reaction following ionization, $(\text{HCOOH})_6 + h\nu \rightarrow [(\text{HCOOH})_6]^+ + e^- \rightarrow (\text{HCOOH})_5\text{H}^+ + \text{HCOO} + e^-$. With the timing delay changes presented in Fig. 4, the mass spectrum of cluster ions indicates that the neutral cluster distribution is different in different parts of the pulsed molecular beam. For example, at a delay time of 170 μs , the neutral cluster distribution at the first part of the molecular beam is detected, and at 200 μs , the distribution at

the middle part of the beam pulse is detected. At the beginning and end of molecular beam, the temperature is higher and expansion pressure is lower than that of the middle part. This means that the neutral cluster $(\text{HCOOH})_6$ is a stable structure in the molecular beam at a relatively low temperature. The $(\text{HCOOH})_5\text{H}^+$ signal also increases with increased backing pressure. A similar behavior is also observed in Feng and Lifshitz's experiments.^{7,8} They found that the intensity of $(\text{HCOOH})_5\text{H}^+$ can be identified as a magic number for low temperature clusters. Thus, the $(\text{HCOOH})_5\text{H}^+$ cluster intensity anomaly is due to the stability of the neutral $(\text{HCOOH})_6$ cluster. This result is different than the intensity anomaly found in water cluster experiments. The relative abundance of cluster $(\text{H}_2\text{O})_{21}\text{H}^+$ is due to the fast metastable fragmentation of $(\text{H}_2\text{O})_{22}\text{H}^+$, not the stability of its parent neutral cluster $(\text{H}_2\text{O})_{22}$, in the molecular beam.³

In the cluster distribution for mixed formic acid/water clusters (Fig. 5), the $\text{H}_2\text{O}(\text{HCOOH})_5\text{H}^+$ cluster is particularly abundant in the mass spectrum, with formic acid serving as a solvent. Based on *ab initio* calculations,¹² the $\text{H}_2\text{O}(\text{HCOOH})_5\text{H}^+$ cluster has a cyclic-type structure, and the H_3O^+ ion core is fully surrounded and stabilized by five formic acid molecules. Additionally, formic acid and water can solvate each other with any ratio of the two species as shown in Figs. 6 and 8.

C. Unimolecular metastable dissociation reactions

Metastable decay [loss of $(\text{HCOOH})_{1,2}$] rate constants for protonated formic acid clusters (outside the ionization/extraction region of the TOFMS, $t > 1 \mu\text{s}$ following ionization) are measured to be about $0.1\text{--}0.8 \times 10^4 \text{ s}^{-1}$. The rates are similar to those of all van der Waals ($0.6\text{--}1.5 \times 10^4$) and hydrogen bonded ($0.1\text{--}2.0 \times 10^4$) cluster ions studied by 26.5 eV single photon photoionization.³⁻⁵ This coincidence implies a loose relation between cluster binding energy, (VIE-AIE), ΔH for proton transfer, and the barriers to the proton transfer reactions in the appropriate clusters. While this is not a quantitative relationship, it is qualitatively implied by the similar rate constants.

An oscillating behavior in the rate constant for odd and even n clusters $(\text{HCOOH})_n\text{H}^+$ is observed, as shown in Fig. 10. The loss of a monomer is more probable for odd number (n odd) clusters and loss of a dimer is more probable for even number (n even) clusters. The observation implies certain structural information for protonated formic acid ion clusters. Note too that these observations imply a slow unimolecular dissociation of the clusters based on only little residual excess energy. The protonated cluster ion series $(\text{HCOOH})_n\text{H}^+$ has been studied through EI.⁷ Following cluster ion generation by EI, unimolecular dissociation is observed. $(\text{HCOOH})_n\text{H}^+$ clusters with $n \leq 5$ are shown to release mainly a monomer. Dimer evaporation is favored for $n \geq 6$ with monomer evaporation effectively disappearing at $n=9$. Metastable rate constants are calculated to be in the range $k = 10^4\text{--}10^6 \text{ s}^{-1}$. Structure for the protonated ion series $(\text{HCOOH})_n\text{H}^+$ is also supported with infrared photodissociation spectroscopy experiments.¹⁰ Reference 10 finds that for clusters $n \leq 6$, the photodissociation spectra show one (n

$= 2, 3$) or two sharp bands ($n=4, 5, 6$) in the free OH stretching vibration region, implying that at least one free OH group is present in each member of the protonated cluster ion series. At $n=7$, the band disappears indicating that the chain is terminated on both ends by cyclic dimers with no free OH moieties in the clusters. Based on *ab initio* calculations of cluster structure,⁹ optimized structures for $n \leq 5$ are found to be open ended chains with one or two free OH group(s) on the ends. Chain structures terminated by cyclic dimer units are favored for $n \geq 6$. The same behavior is found for protonated acetic acid clusters using IR plus vacuum ultraviolet spectroscopy.²²

Neutral cluster $[(\text{HCOOH})_{n+1}]$ structure calculations^{18-21,23} and experiments²⁴ have shown much different results than for the protonated ion series $(\text{HCOOH})_n\text{H}^+$. Neutral clusters form a cyclic structure, with all OH groups involved in the cluster hydrogen bonding network. DFT^{19,21} calculations have yielded trimer structure with the lowest energy structure consisting of the cyclic dimer bonded to a monomer by an $\text{O-H}\cdots\text{O}$ and a $\text{C-H}\cdots\text{O}$ bond. The tetramer has seen more variety in the lowest energy structure for different computational schemes. It is argued that the lowest energy of the tetramer contains a pair of dimers held together by two weak $\text{C-H}\cdots\text{O}$ bonds,^{20,21} with several other structures lying within 0.4 kcal/mol. Limited attention has been paid to the neutral pentamer for which the Gibbs free energy suggests that the most stable structure is a planar ring that consists of the lowest energy trimer bound to the lowest energy dimer by two $\text{C-H}\cdots\text{O}$ bonds.²¹ The general trend, for neutral formic acid clusters $n \leq 5$, seems to be that the lowest energy structures favor rings or chains made up of the lowest energy dimers and trimers, in combination with monomers, not open ended monomer chains, or monomer chains terminated by cyclic dimers, as suggested for the protonated ion cluster series $(\text{HCOOH})_n\text{H}^+$.

Figures 9 and 10 present results of metastable fragmentation of protonated formic acid clusters after ionization by the 26.5 eV soft x-ray laser. In the range of $5 \leq n \leq 9$, our results follow closely those generated by the EI experiments;⁷ that is, loss of a dimer is favored over a monomer. A more obvious alternating behavior corresponding to odd and even clusters is observed in our experiments. Additionally, at cluster size $n=4$, our results differ from those generated by EI. 26.5 eV single photon ionization for $(\text{HCOOH})_4\text{H}^+$ yields dimer evaporation as nearly the only open channel. Conversely, EI demonstrates only monomer evaporation for $(\text{HCOOH})_4\text{H}^+$. These different metastable dissociation reactions indicate a different structure for the parent ion of the protonated formic acid cluster $(\text{HCOOH})_4\text{H}^+$. This could be caused by different ionization processes and different generation conditions for the clusters.

One can also note this structural difference in values of metastable dissociation rate constants for EI and single photon ionization generated species. Metastable decay rates are calculated to be in the range of $0.1\text{--}0.8 \times 10^4 \text{ s}^{-1}$ for ionization upon a single 26.5 eV photon, whereas EI rate constants are almost three orders of magnitude faster in the range $k = 10^4\text{--}10^6 \text{ s}^{-1}$. This distinction could arise from the difference in energy deposited into the cluster from a 26.5 eV

photon and an electron beam. A single 26.5 eV photon deposits very little (excess) energy in the cluster after ionization for fragmentation. Since clusters under ionization by EI have much faster metastable decay rates, these clusters must be hotter with more energy deposited in the cluster for metastable fragmentation than those created by 26.5 eV single photon ionization.

If the EI generated cluster ion is hotter and has more energy than the single photon generated cluster ion, its structural properties and its position on its potential energy surface can be different. For example, the most stable structure of neutral cluster $(\text{HCOOH})_5$ as suggested by calculations²¹ is a ring structure consisting of two dimers and one monomer. During the ionization process, the excess energy deposited in the cluster may cause it to break apart into an open chain structure. After EI ionization, the protonated cluster ion $(\text{HCOOH})_4\text{H}^+$, generated from the neutral cluster $(\text{HCOOH})_5$ by a proton transfer reaction following ionization, may have an open chain structure without any dimer rings;⁹ evaporation of single monomer is thus a favorable process for the metastable dissociation of EI generated $(\text{HCOOH})_4\text{H}^+$. After ionization by a single 26.5 eV photon, however, the photoelectron takes away almost all of the energy above the vertical ionization energy leaving little excess energy in the cluster. The structure of this cluster ion generated by photoionization may be much different than the structure of the ion generated by EI, and indeed may still have the structure of its neutral parent. Neutral formic acid clusters are of the general form of rings or chains consisting of lowest energy dimers and trimers. Thus, under appropriate experimental conditions, the metastable loss of a dimer following ionization and the proton transfer reaction is not unreasonable, even for $(\text{HCOOH})_4\text{H}^+$.

Another reason for the difference between EI and photoionization generated ions is that a number of isomers exist for protonated clusters, which depend on the neutral cluster generation conditions and ionization method. The internal energy for cool or hot clusters generated by photoionization or EI will be used for the proton transfer reaction, structure change, and metastable fragmentation following ionization. Protonated formic acid clusters have a number of different isomeric structures with similar energies, such as open chain, and one or two dimers at the end of a cluster chain.⁷⁻¹⁰ Feng and Lifshitz's EI experiments⁷ show that low temperature favors dimer loss, while high temperature favors monomer loss; high temperature will supply more internal energy for cluster structural rearrangement to totally opened chains after ionization. Of course, more energy deposited by the ionization process can also generate the result that monomer loss becomes favorable for small protonated formic acid clusters.

V. CONCLUSIONS

Pure neutral $(\text{HCOOH})_{n+1}$ clusters and $(\text{HCOOH})/(\text{H}_2\text{O})$ mixed clusters are investigated by TOFMS employing single photon, 26.5 eV ionization. For the pure HCOOH system, the dominant cluster series in the mass spectrum is $(\text{HCOOH})_n\text{H}^+$ which is directly generated from ionization of neutral clusters $(\text{HCOOH})_{n+1}$ in the mo-

lecular beam and a proton transfer reaction. Clusters are observed for $2 < n < 15$ with an intensity anomaly at $n=5$. We argue that the intensity anomaly at $(\text{HCOOH})_5\text{H}^+$ is due to the enhanced stability of the $(\text{HCOOH})_6$ neutral cluster and not an enhanced metastable fragmentation rate for $(\text{HCOOH})_6\text{H}^+$ as found for $(\text{H}_2\text{O})_{21}\text{H}^+$ and $(\text{H}_2\text{O})_{22}\text{H}^+$ clusters. The neutral dimer and larger cluster structures are determined to involve cyclic dimers with the absence of any free OH bonds since the channel of OH loss, which is the main channel for dissociation following photoionization for the formic acid monomer, is not observed by 26.5 eV laser photoionization. The $\text{H}^+(\text{HCOOH})_{n-1}\text{CH}_2$ cluster ion series is observed (weakly) as a dissociation product following photoionization of neutral $(\text{HCOOH})_{n+1}$ clusters. This reaction channel must open for a highly excited state of the ion. This fragmentation pathway is relatively weak ($< 10\%$) compared to the parent ion $(\text{HCOOH})_n\text{H}^+$ signal because in most instances, all of the excess cluster energy above VIE is removed by the photoelectron during the ionization process.

Mixed HCOOH/ H_2O clusters are studied at two different HCOOH concentrations mixed with water and two different expansion gas pressures. The predominant signals in the mass spectra are $(\text{HCOOH})_n\text{H}^+$ and $(\text{HCOOH}) \times (\text{H}_2\text{O})_m\text{H}^+$ cluster ions for high and low parameter values, respectively. For the high concentration condition a magic number at $n=5$, $m=1$ for the protonated cluster ion series $(\text{HCOOH})_n(\text{H}_2\text{O})_m\text{H}^+$ is found.

For the hydrogen bonded protonated cluster ion series $(\text{HCOOH})_n\text{H}^+$, metastable dissociation by loss of one or two HCOOH molecules from the cluster is observed in the reflectron TOF mass spectrum for 26.5 eV single photon ionization. The metastable dissociation rate constants are in the range of $(0.1-0.8) \times 10^4 \text{ s}^{-1}$ for $4 < n < 9$. This is the same range as observed for the comparable dissociation of $(\text{CO}_2)_n^+$, $(\text{SO}_2)_n^+$, $(\text{H}_2\text{O})_n\text{H}^+$, $(\text{CH}_3\text{OH})_n\text{H}^+$, and $(\text{NH}_3)_n\text{H}^+$ clusters. This similarity between rate constants for many van der Waals and hydrogen bonded clusters implies that cluster dynamics is dependent upon cluster density of states and internal cluster temperature. An obvious oscillating behavior is observed for metastable fragmentation of protonated formic acid clusters after single photon ionization, indicating a cluster ion structure with both dimer and monomer units in the neutral cluster.

In general, $(\text{HCOOH})_n\text{H}^+$ clusters are observed with a gentle ionization source (soft x-ray laser) that is capable of ionizing the clusters with a single photon. This gentle ionization allows us to obtain data about the protonated cluster ion series $(\text{HCOOH})_n\text{H}^+$ distribution and we argue that it is similar to the neutral cluster distribution of formic acid.

ACKNOWLEDGMENTS

This research has been supported in part by the NSF ERC for Extreme Ultraviolet Science and Technology under NSF Award No. 0310717 and grants from Philip Morris USA and the National Science Foundation.

¹S. D. Rodgers and S. Charnley, *Mon. Not. R. Astron. Soc.* **320**, L61 (2001).

²I. Martin, T. Skalicky, J. Langer, H. Abdoul-Carime, G. Karwasz, E.

- Illengerger, M. Stano, and S. Matejcik, *Phys. Chem. Chem. Phys.* **7**, 2212 (2005).
- ³F. Dong, S. Heinbuch, J. J. Rocca, and E. R. Bernstein, *J. Chem. Phys.* **124**, 224319 (2006).
- ⁴F. Dong, S. Heinbuch, J. J. Rocca, and E. R. Bernstein, *J. Chem. Phys.* **125**, 154317 (2006).
- ⁵S. Heinbuch, F. Dong, J. J. Rocca, and E. R. Bernstein, *J. Chem. Phys.* **125**, 154316 (2006).
- ⁶F. Dong, S. Heinbuch, J. J. Rocca, and E. R. Bernstein, *J. Chem. Phys.* **125**, 164318 (2006).
- ⁷W. Y. Feng and C. Lifshitz, *J. Phys. Chem.* **98**, 6075 (1994).
- ⁸C. Lifshitz and W. Y. Feng, *Int. J. Mass Spectrom. Ion Process.* **146**, 223 (1995).
- ⁹R. Zhang and C. Lifshitz, *J. Phys. Chem.* **100**, 960 (1996).
- ¹⁰Y. Inokuchi and N. Nishi, *J. Phys. Chem.* **107**, 11319 (2003).
- ¹¹V. Aviyente, R. Zhang, T. Varnali, and C. Lifshitz, *Int. J. Mass Spectrom. Ion Process.* **161**, 123 (1997).
- ¹²Y. Inokuchi and N. Nishi, *J. Phys. Chem. A* **106**, 4529 (2002).
- ¹³S. Heinbuch, M. Grisham, D. Martz, and J. J. Rocca, *Opt. Express* **13**, 4050 (2005).
- ¹⁴J. J. Rocca, V. N. Shlyaptsev, F. G. Tomasel, O. D. Cortazar, D. Hartshorn, and J. L. A. Chilla, *Phys. Rev. Lett.* **73**, 2192 (1994).
- ¹⁵B. R. Benware, C. D. Macchietto, C. H. Moreno, and J. J. Rocca, *Phys. Rev. Lett.* **81**, 5804 (1998).
- ¹⁶H. Su, Y. He, F. Kong, W. H. Fang, and R. Z. Liu, *J. Chem. Phys.* **113**, 1891 (2000); R. S. Irwin, D. L. Singleton, C. Paraskevopoulos, and R. McLaren, *Int. J. Chem. Kinet.* **26**, 219 (1994); T. Ebata, T. Amano, and M. Ito, *J. Chem. Phys.* **90**, 112 (1989); L. Khriachtchew, E. Macoas, and M. Rasanen, *J. Am. Chem. Soc.* **124**, 10994 (2002).
- ¹⁷J. S. Francisco, *J. Chem. Phys.* **96**, 1167 (1992).
- ¹⁸A. Allouche, *J. Chem. Phys.* **122**, 234703 (2005).
- ¹⁹A. K. Roy and A. J. Thakkar, *Chem. Phys. Lett.* **386**, 162 (2004).
- ²⁰Y. Zhao and D. G. Truhlar, *J. Phys. Chem. A* **109**, 6624 (2005).
- ²¹A. K. Roy and A. J. Thakkar, *Chem. Phys.* **312**, 119 (2005).
- ²²Y. J. Hu, H. B. Fu, and E. R. Bernstein, *J. Chem. Phys.* **125**, 184308 (2006).
- ²³A. Karpfen and A. J. Thakkar, *J. Chem. Phys.* **124**, 224313 (2006).
- ²⁴J. Karle and L. O. Brockway, *J. Am. Chem. Soc.* **66**, 574 (1944); A. Almennigen, O. Bastiansen, and T. Motzfeldt, *Acta Chem. Scand.* (1947-1973) **23**, 2848 (1969); **24**, 747 (1970).